有機化学への応用

WORK

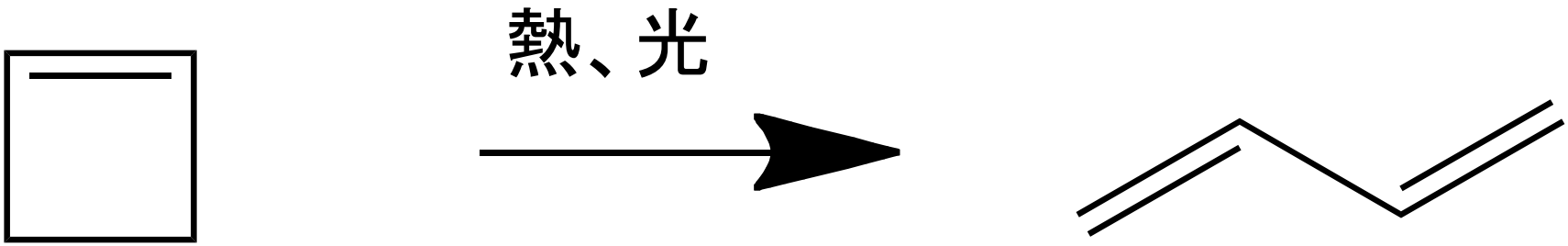

?

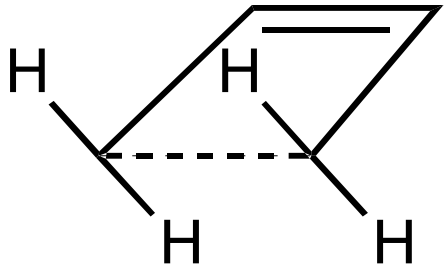

同旋
conrotatory

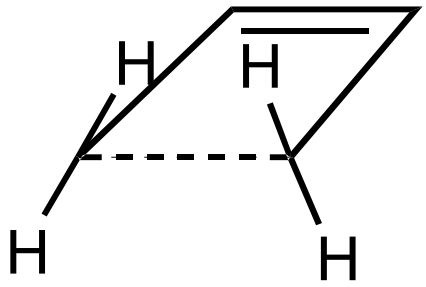

逆旋
disrotatory

有機化学への応用

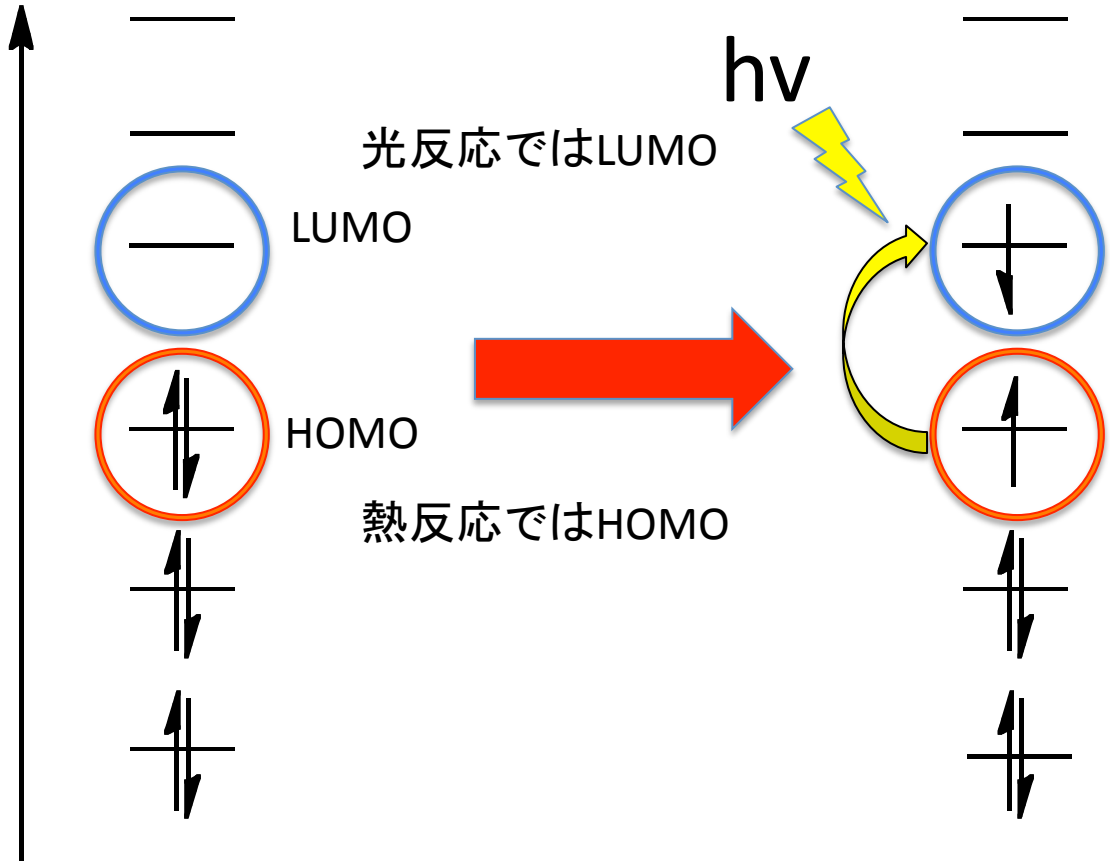

有機化学への応用

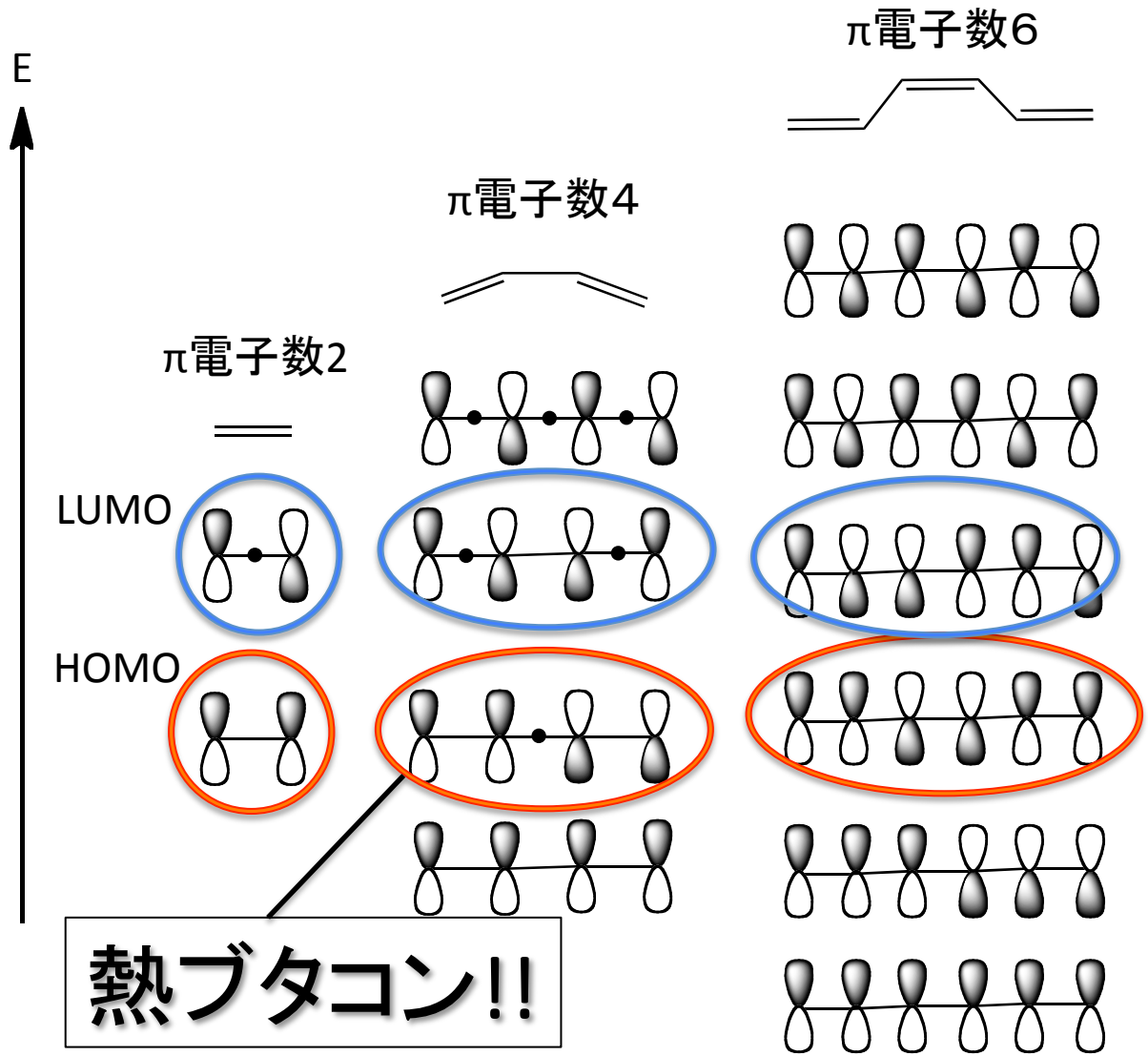

位相が合うように回転
両端同位相→　逆旋
両端逆位相→　同旋

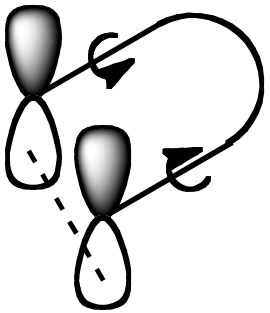

逆旋
disrotatory

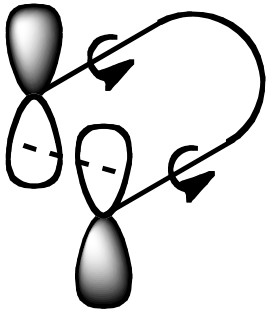

同旋
conrotatory

有機化学への応用-8

WORK

2＋2

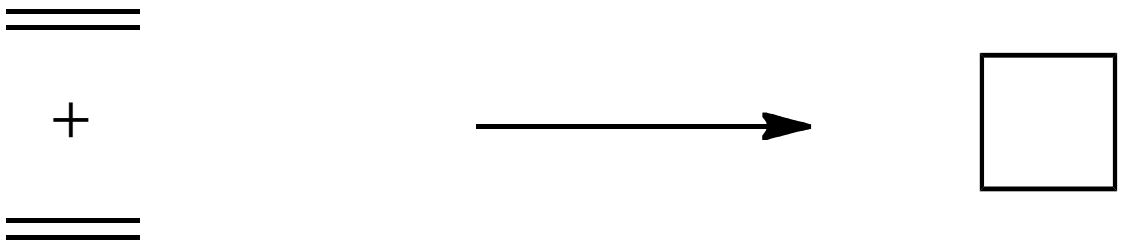

2＋4

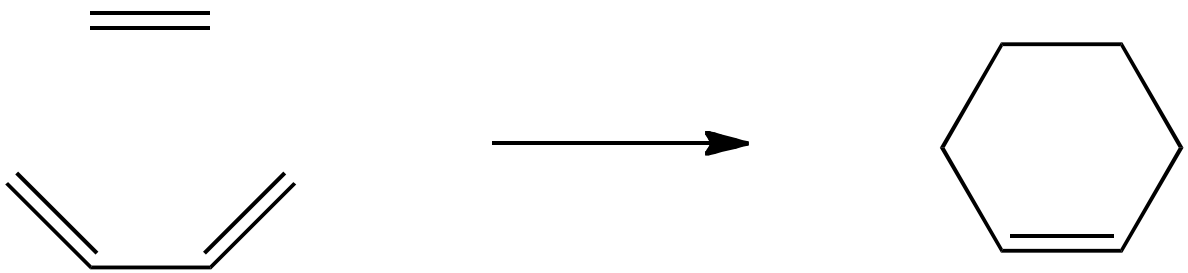

有機化学への応用

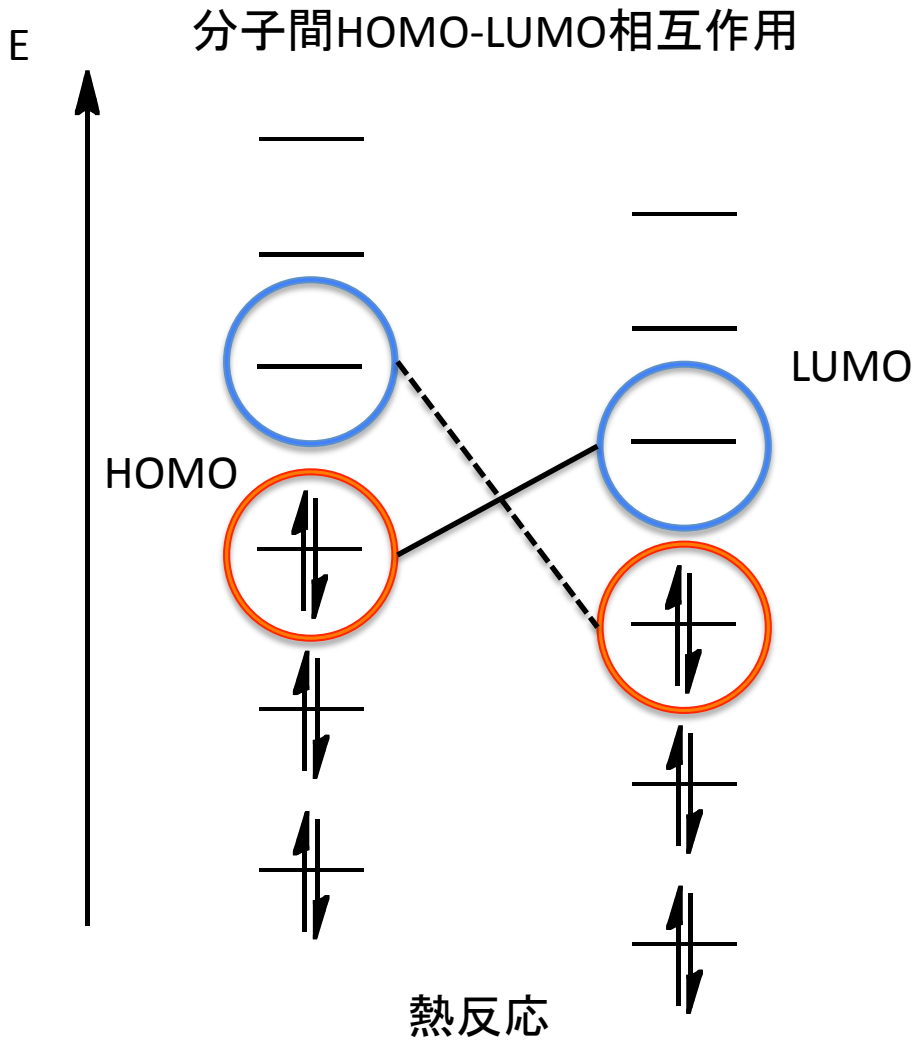
E
分子間HOMO-LUMO相互作用
LUMO
HOMO
熱反応

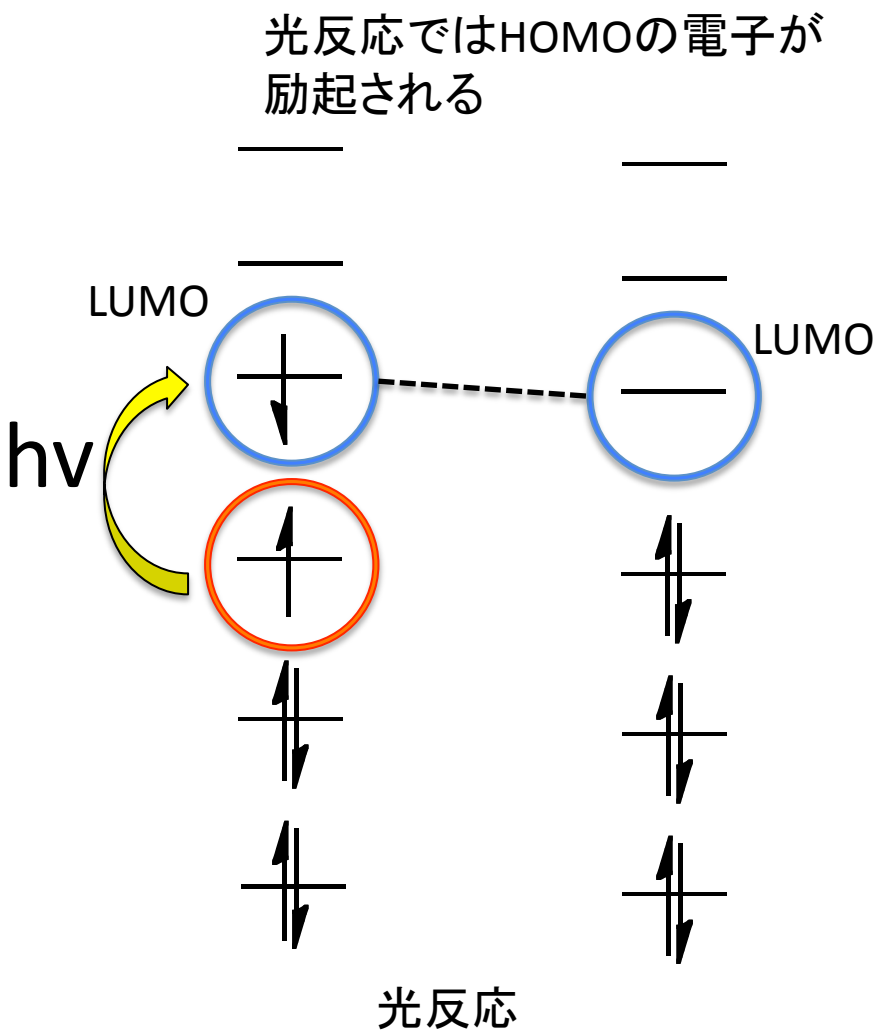
光反応ではHOMOの電子が
励起される
LUMO
LUMO
hv
光反応

有機化学への応用

分子軌道の位相が合えば協奏的ç

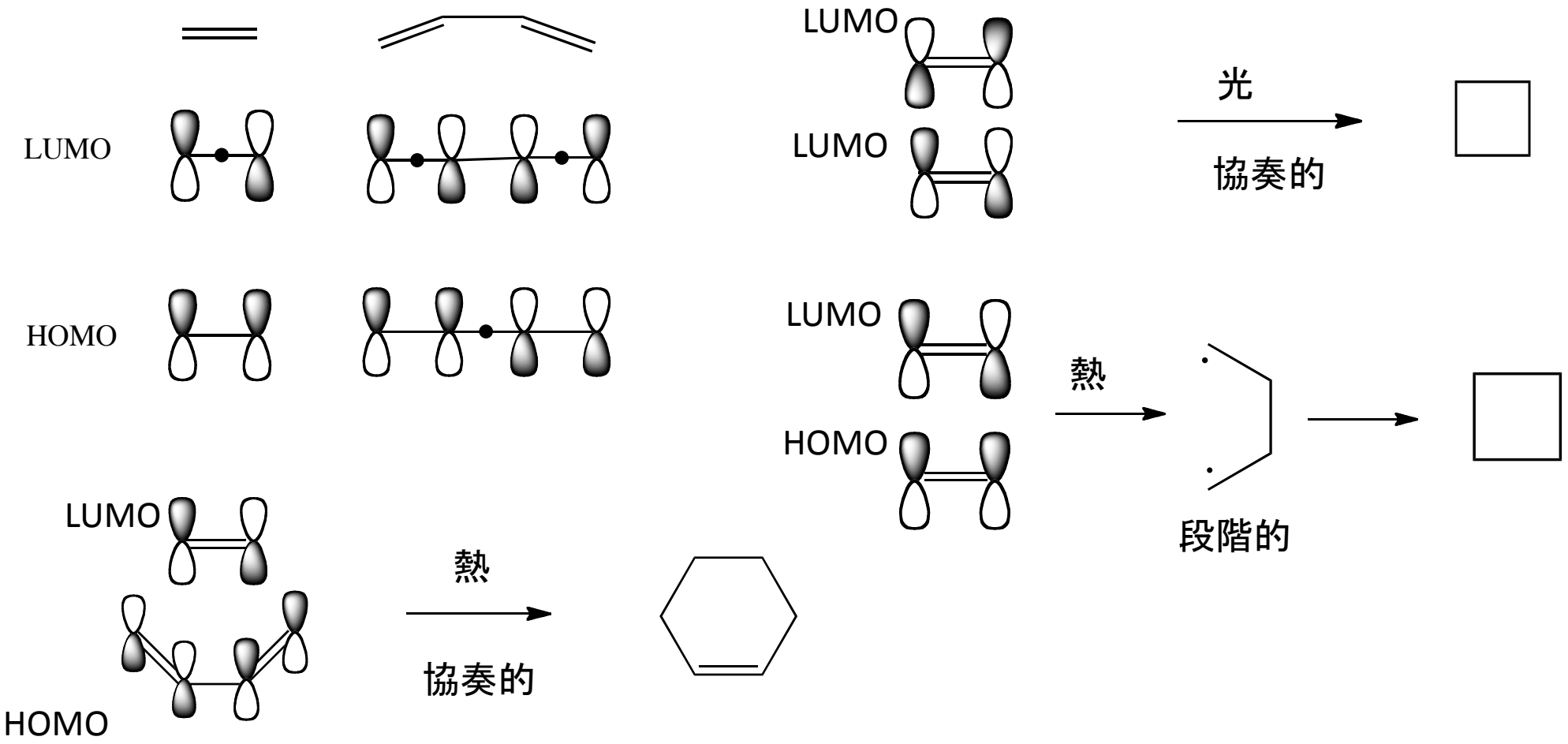

有機化学への応用

キレトロピー反応　→　二つの部位にわけて考える

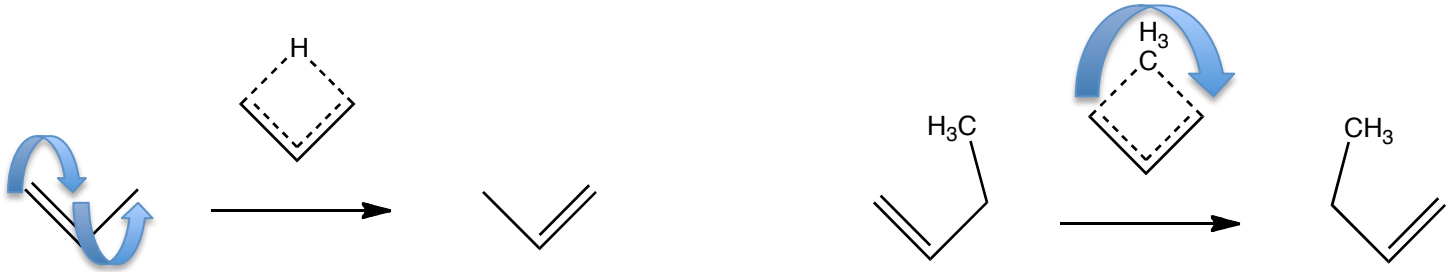

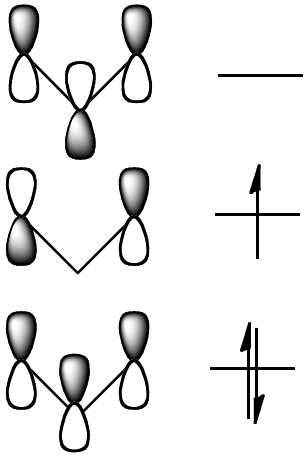

H転移

メチル転移

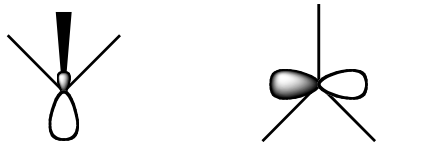

立体保持　　立体反転

有機化学への応用

Transition Structures of Hydrocarbon Pericyclic Reactions
K. N. Houk, Y. Li, and J. D. Evanseck

Twenty-five years after the discovery of a vast class of organic reactions named “pericyclic reactions” by Woodward and Hoffmann, ab initio quantum mechanics provides a detailed analysis of the geometries, energies, and electronic characteristics of the transition structures of these reactions. Common features are found in all these reactions, and generalizations permit prediction of other transition-structure geometries and energies. At the same time, great diversity is observed-from strongly bonded, rigid, closed-shell entities to weakly interacting, flexible diradical structures.

Angew,. Chem. Int. Ed. Engl. **31**, 682- 708 (1992)

この論文はWH則が発見されてから25年後にでました。
この論文からさらに25年たちました。

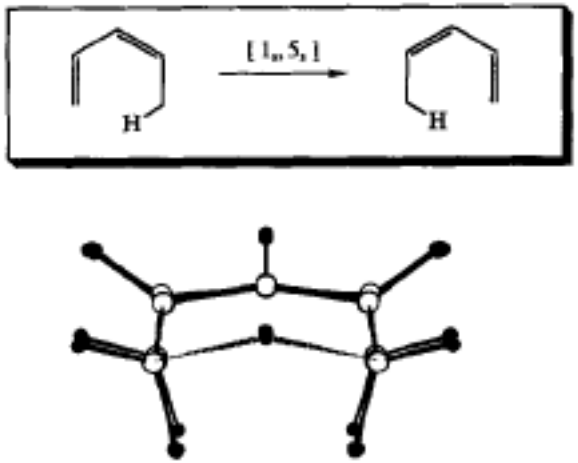

Fig. 6. Superimposed transition structures of the [1,5] sigmatropic hydrogen shift in pentadiene obtained with AM-1, STO-3G, 3-21G, 6-31G, 6-31G*, 6-31G**, MP2/3-21G, and MP2/6-31G* methods.

WORK

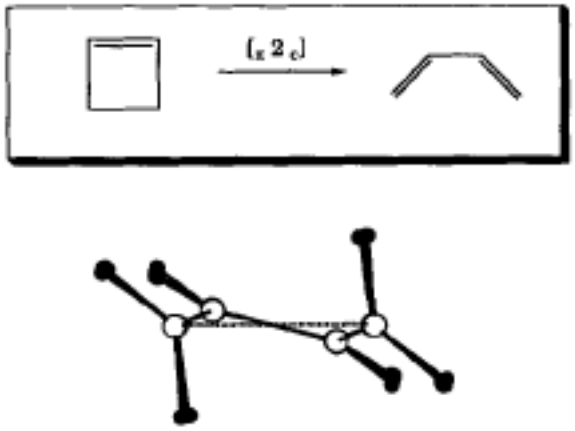

Fig. 7. Superimposed transition structures the electrocyclic ring opening of cyclobutene obtained with AM-1, STO-3G, 3-21G, 4-31G, 6-31G, 6-31G*, 6-31G**, MP2/3-21G, and MP2/6-31G* methods.

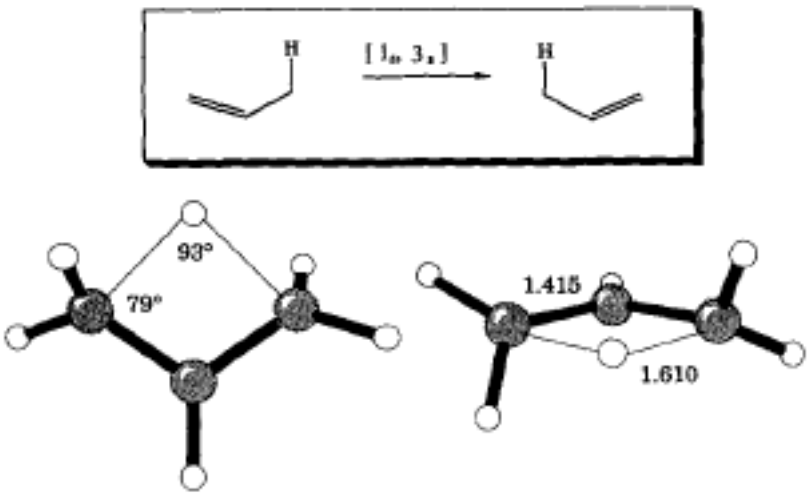

Fig. 9. Two views of the CASSCF/6-31G* transition structure of the [1s,3s] sigmatropic hydrogen shift in propene (J. W. Storer).

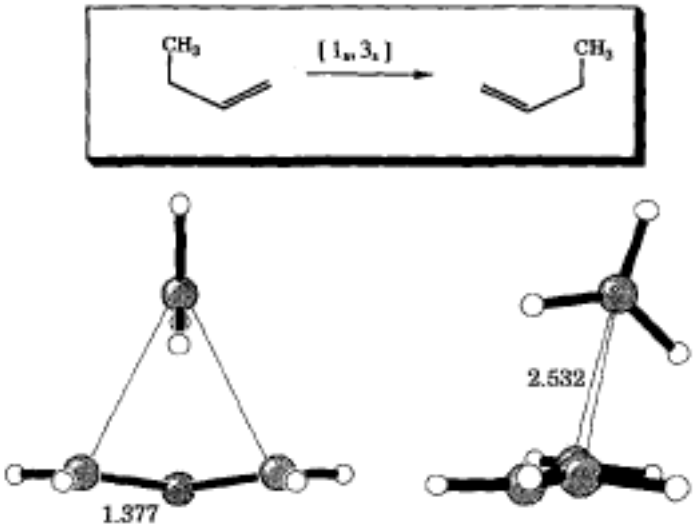

Fig. 10. The RHF/3-21G transition structures of the [1s,3s] sigmatropic methyl shift in 1-butene (J. W. Storer).

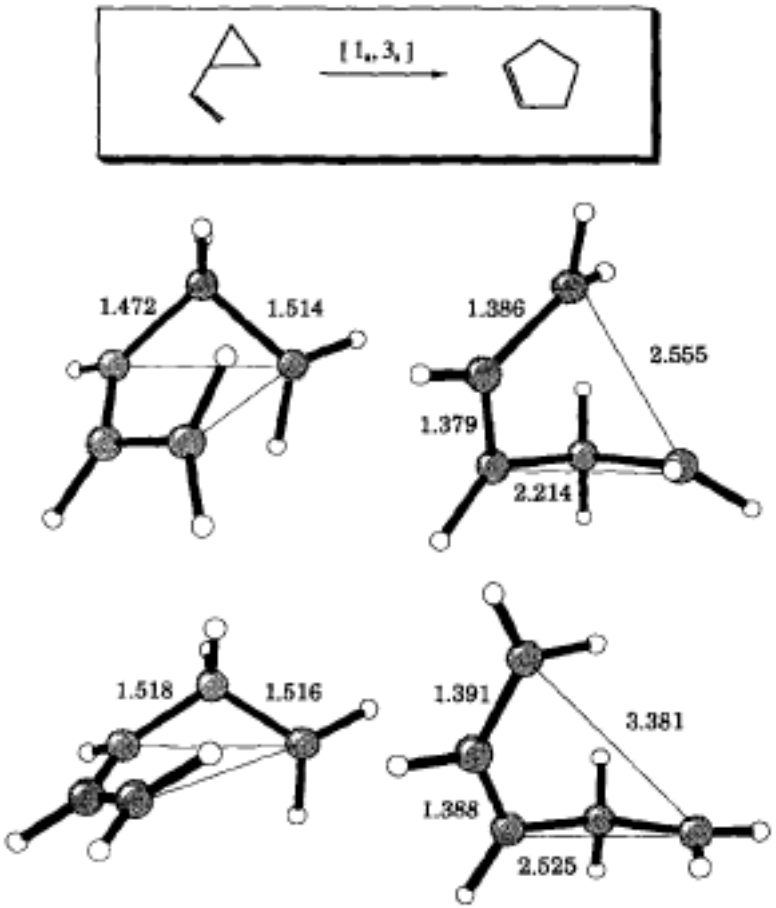

Fig. 11. The RHF/6-31G* (top) and of the CASSCF/3-21G transition structures (bottom) of [1s,3s] sigmatropic vinylcyclopropane–cyclopentene shift (J. W. Storer).

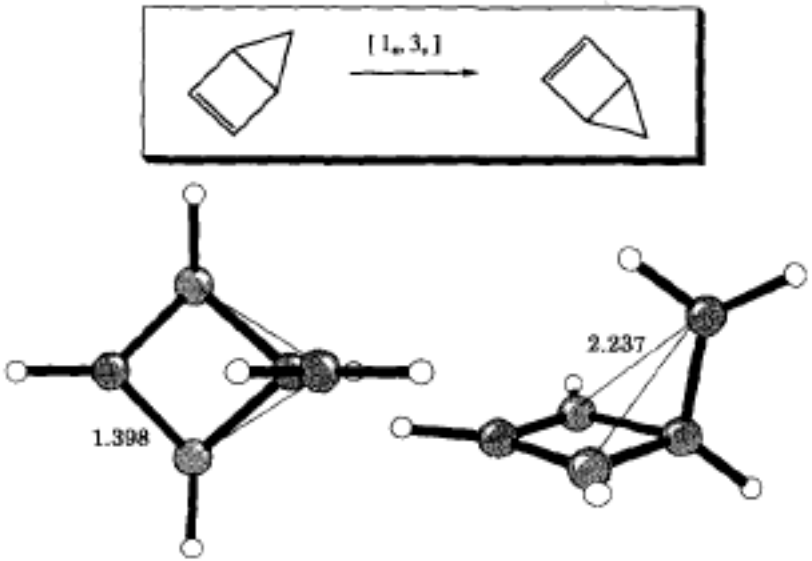

Fig. 12. The RHF/3-21G transition structure of [1s,3s] sigmatropic methylene shift in bicyclo[2.1.0]pentene [69a].

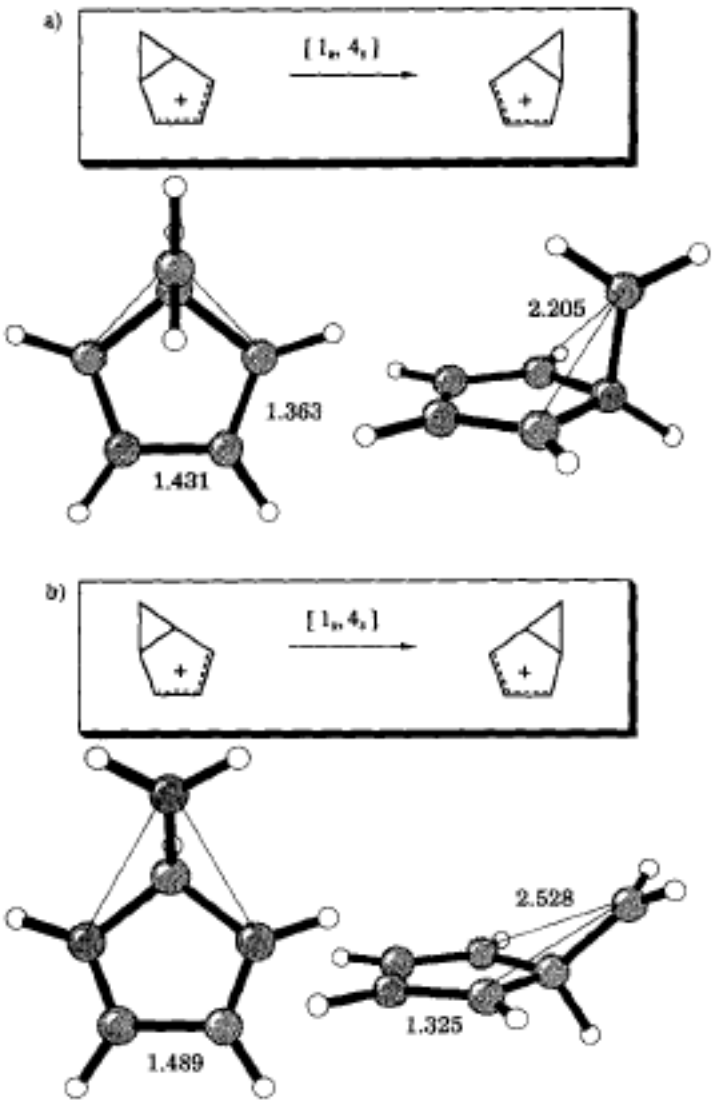

Fig. 14. The RHF/3-21G transition structures of the [1,4] sigmatropic methylene shift in bicyclo[3.1.0]hexenyl cation (S. M. Ernst): a) the $[1_s,4_s]$ pathway; b) the $[1_s,4_s]$ pathway.

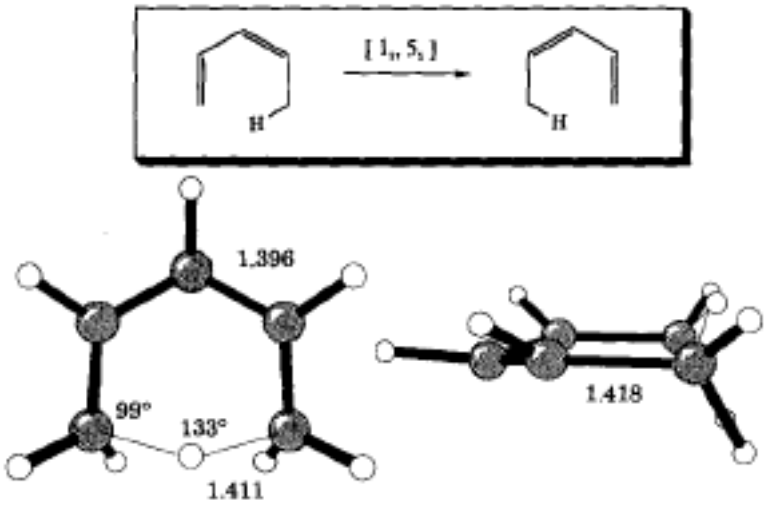

Fig. 15. The MP2/6-31G* transition structure of the $[1_s,5_s]$ sigmatropic hydrogen shift in pentadiene [39a].

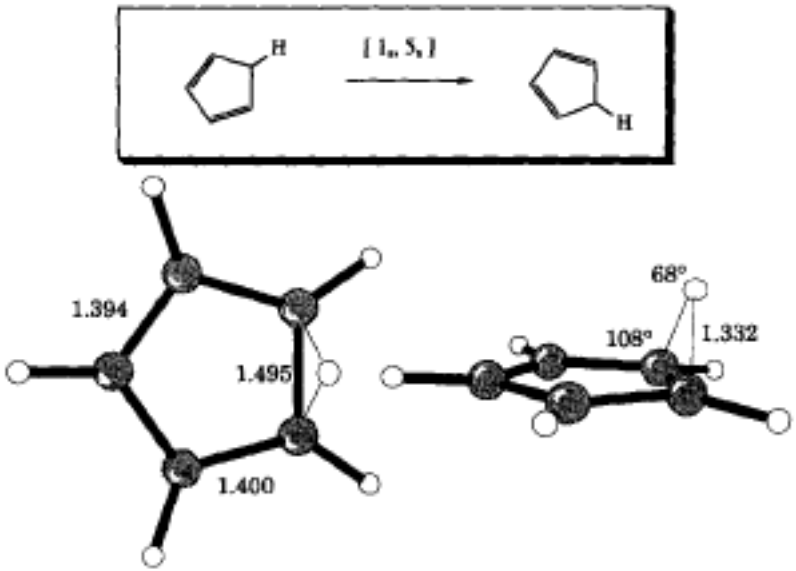

Fig. 16. The RHF/3-21G transition structure of the $[1_s,5_s]$ sigmatropic hydrogen shift in cyclopentadiene [39c].

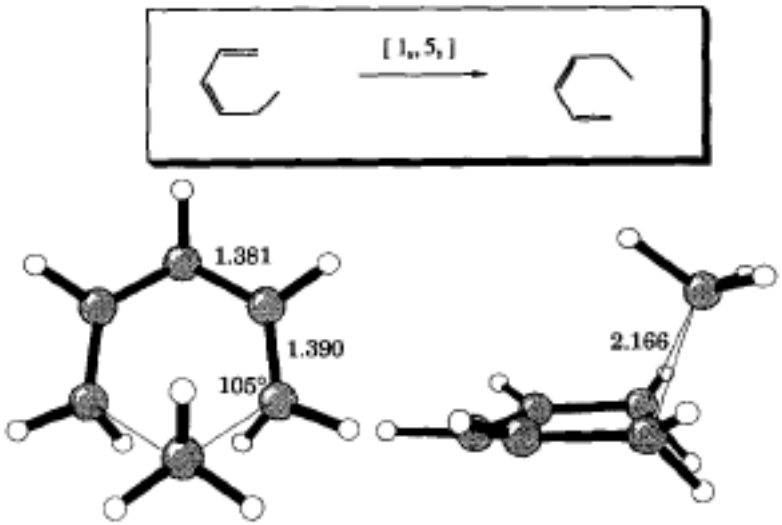

Fig. 17. The RHF/3-21G transition structure of the [1s,5s] sigmatropic methyl shift in *cis*-1,3-hexadiene (F. Jensen).

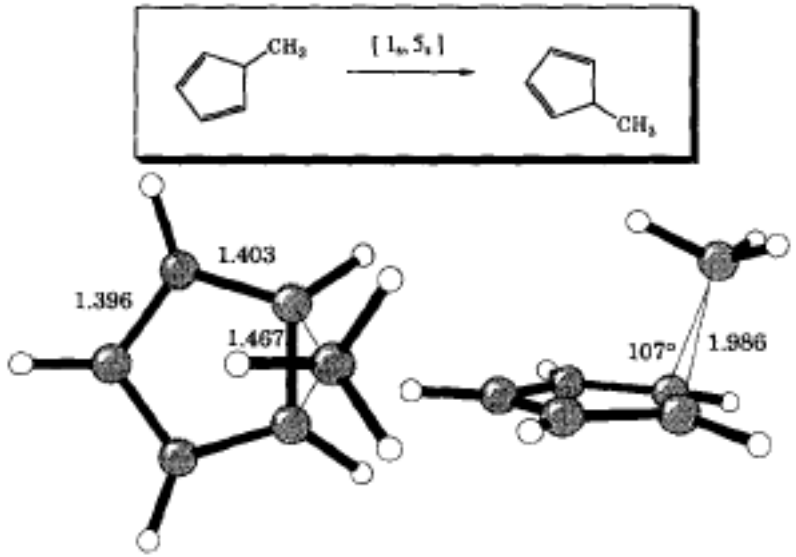

Fig. 18. The RHF/3-21G transition structure of the [1s,5s] sigmatropic methyl shift in methylcyclopentadiene (F. Jensen).

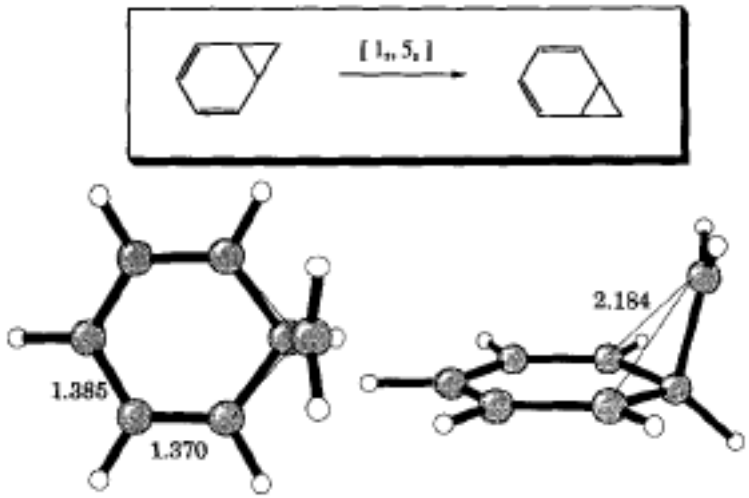

Fig. 19. The RHF/3-21G transition structure of the [1s,5s] sigmatropic methylene shift in norcaradiene (S. M. Ernst).

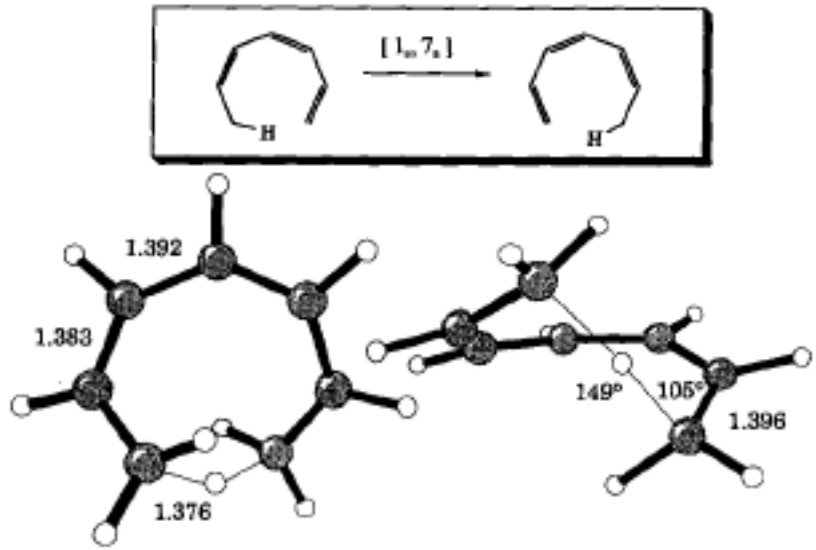

Fig. 20. The RHF/3-21G transition structure of the [1s,7s] sigmatropic hydrogen shift in heptatriene [38].

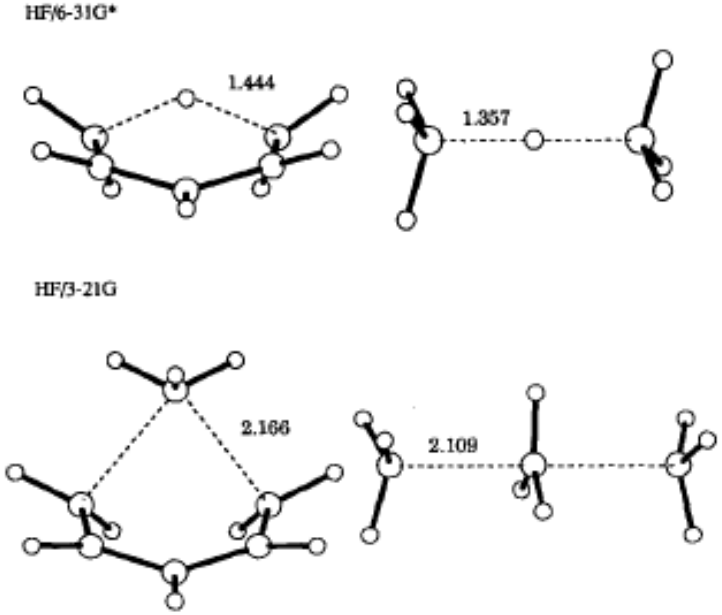

Fig. 21. Comparison of the 6-31G* transition structures of sigmatropic hydrogen shifts with intermolecular hydrogen transfer (top) and the 3-21G transition structures of sigmatropic methyl shifts with intermolecular methyl transfer (bottom).

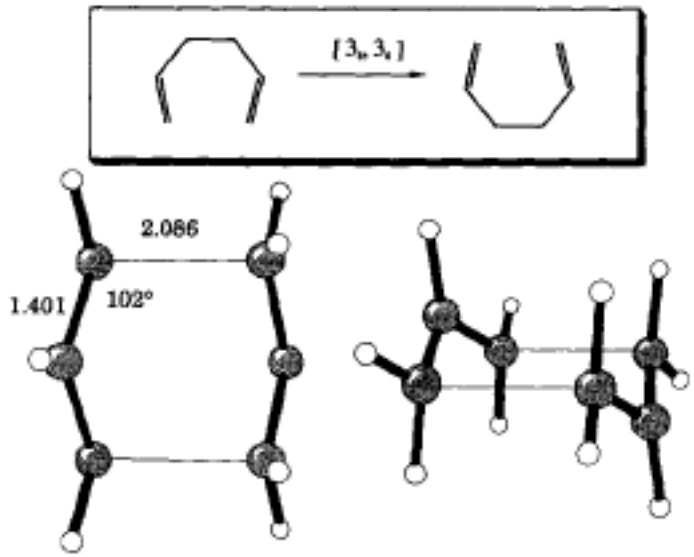

Fig. 22. The CASSCF/3-21G transition structure of [3s,3s] sigmatropic shift (Cope rearrangement) of 1,5-hexadiene [79].

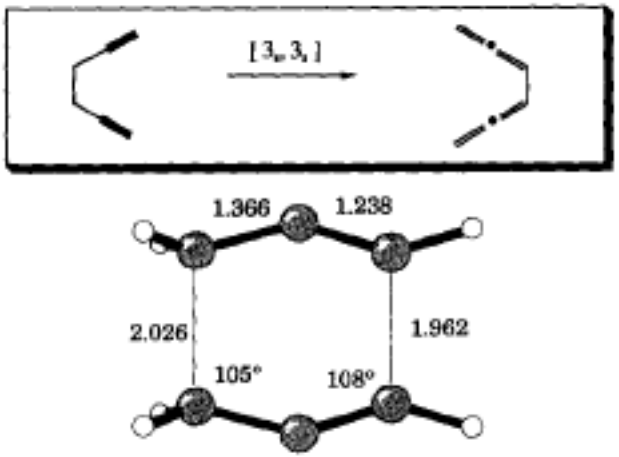

Fig. 23. The RHF/3-21G transition structure of [3s,3s] sigmatropic shift 1,5-hexadiyne (S. M. Ernst and K. Black).

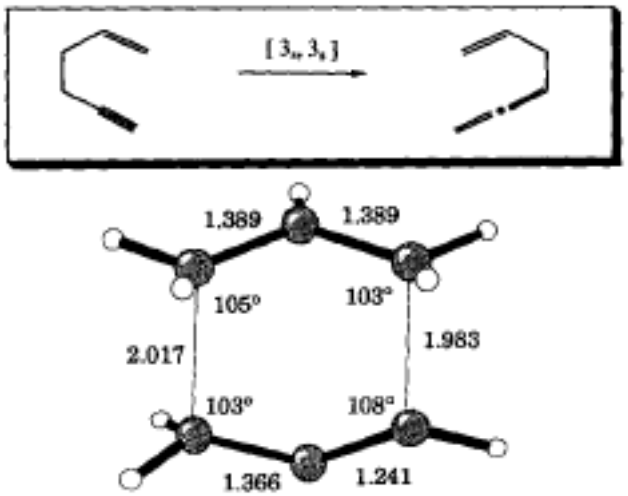

Fig. 25. The RHF/3-21G transition structure of [3s,3s] sigmatropic shift of hex-1-en-5-yne (S. M. Ernst and K. Black).

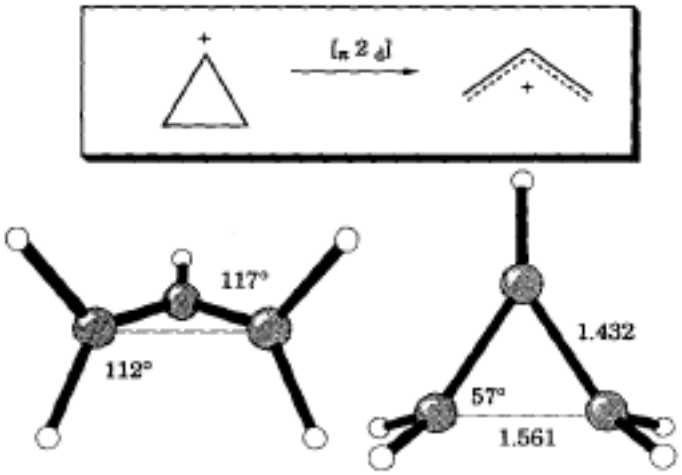

Fig. 28. The MP2/6-31G* transition structure of disrotatory electrocyclic ring opening of the cyclopropyl cation [93]. In this and subsequent drawings of electrocyclic reactions, the angles between the inward and outward rotating hydrogens and the breaking or forming single bond are given.

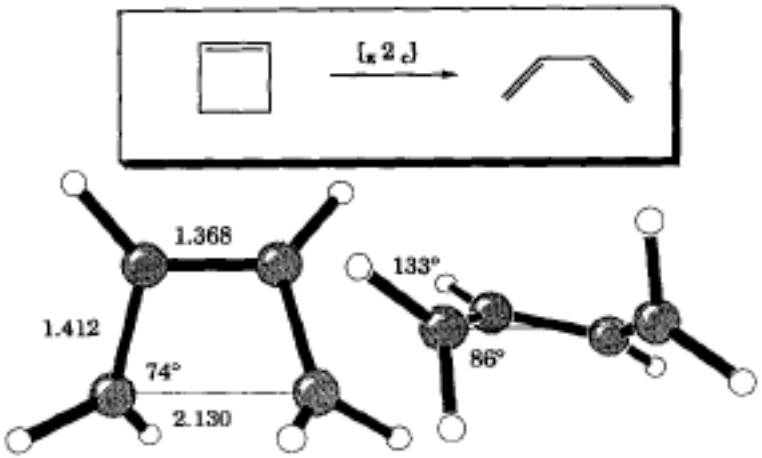

Fig. 30. The MP2/6-31G* transition structure of conrotatory electrocyclic ring opening of cyclobutene [44a].

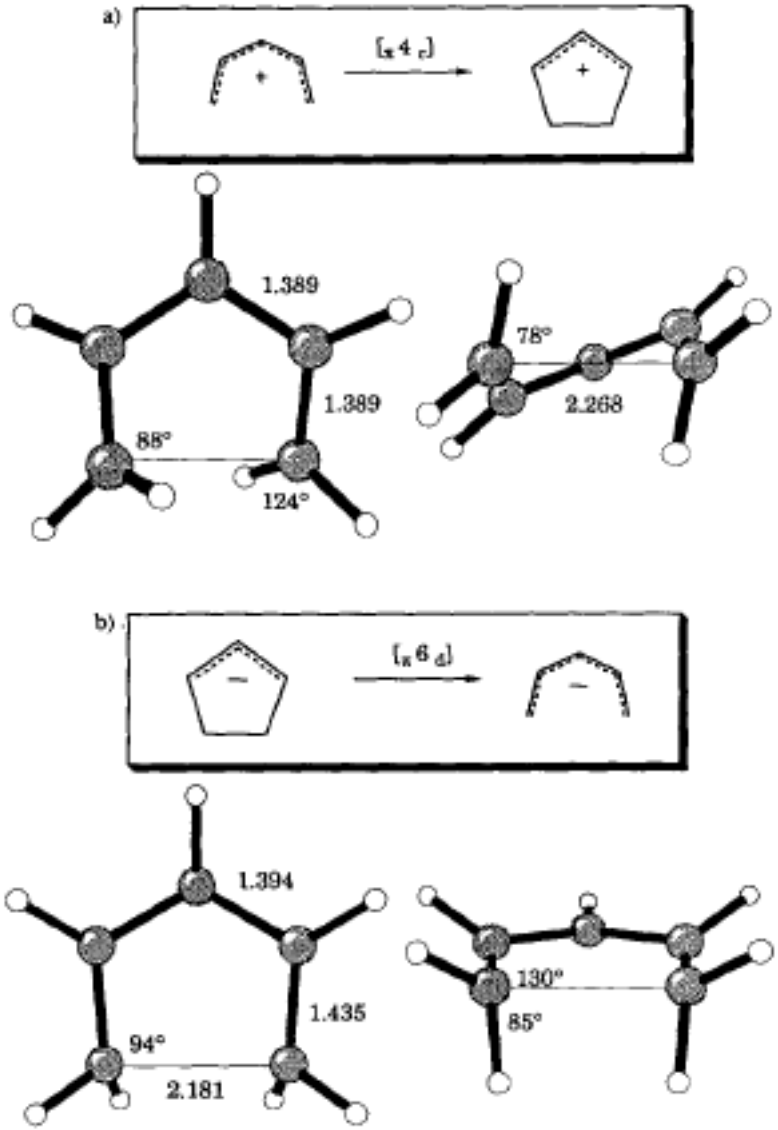

Fig. 32. a) The MP2/6-31G* transition structure of electrocyclization of the pentadienyl cation (E. A. Kallel). b) The RHF/6-31 + G* transition structure of cyclopentenyl anion electrocyclic ring opening (J. D. Evanseck).

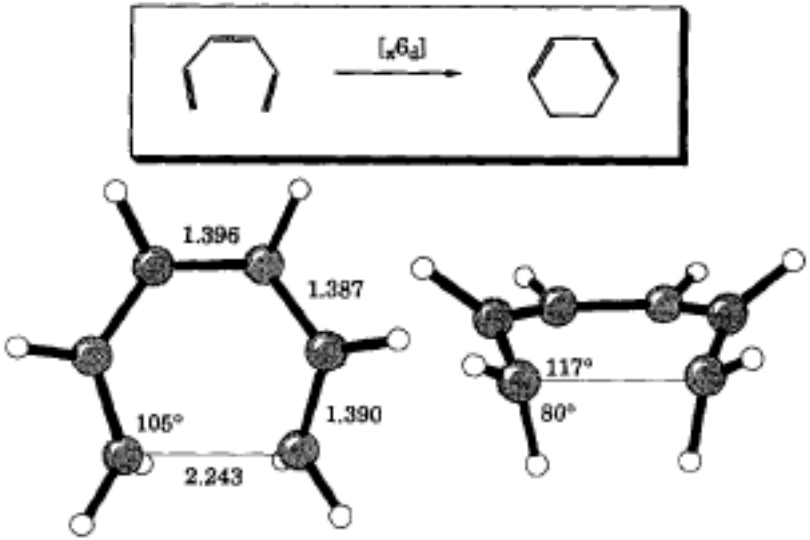

Fig. 33. The RHF/6-31G* transition structure of disrotatory electrocyclization of hexatriene [99].

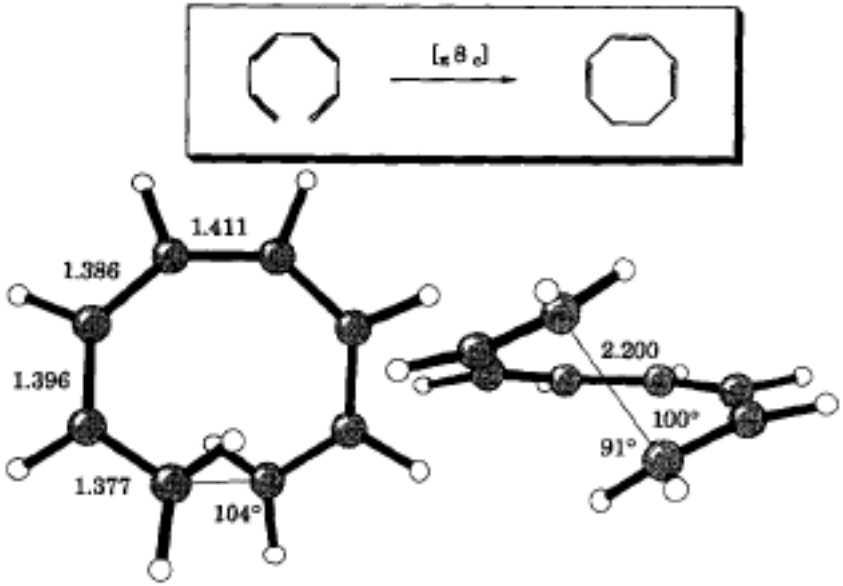

Fig. 35. The RHF/6-31G* transition structure of conrotatory electrocyclic ring opening of cyclooctatriene (J. D. Evanseck).

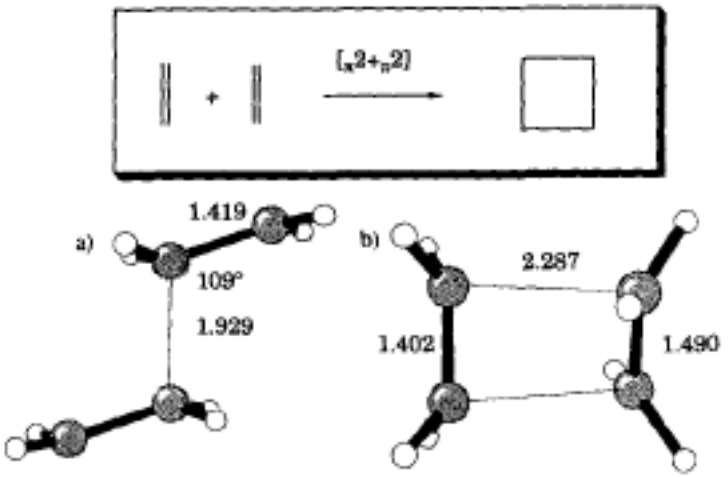

Fig. 41. The MCSCF/3G transition structures of the cyclodimerization of ethene [119b]. a) The nonconcerted [πs2 + πs2] reaction; b) the concerted [πs2 + πs2] reaction.

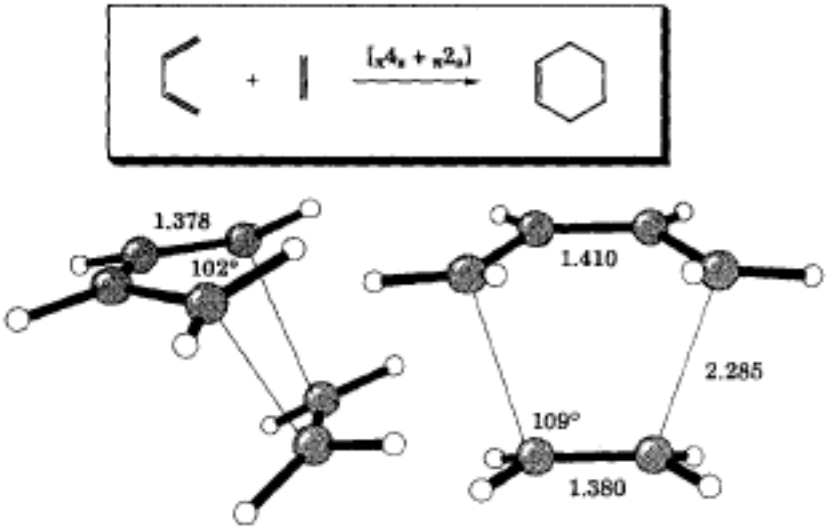

Fig. 43. The MP2/6-31G* transition structure of [πs4 + πs2] cycloaddition between butadiene and ethene (R. J. Loncharich).

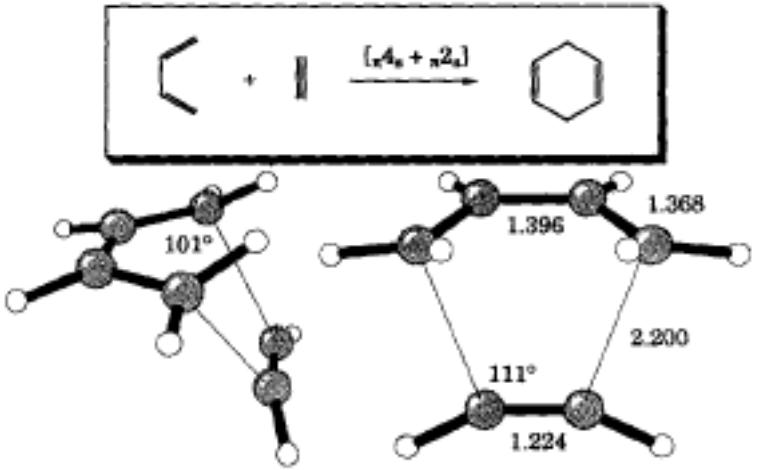

Fig. 44. The RHF/3-21G transition structure of [πs4 + πs2] cycloaddition between butadiene and acetylene (M. McCarrick).

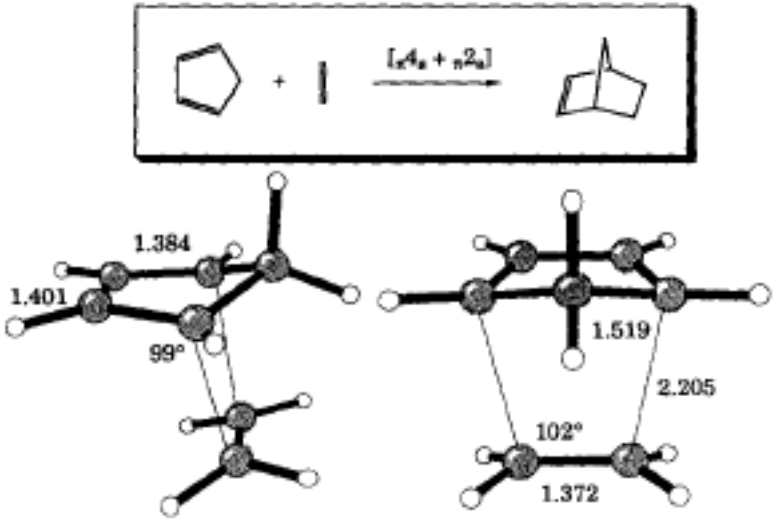

Fig. 45. The RHF/3-21G transition structure of [πs4 + πs2] cycloaddition between cyclopentadiene and ethene [126].

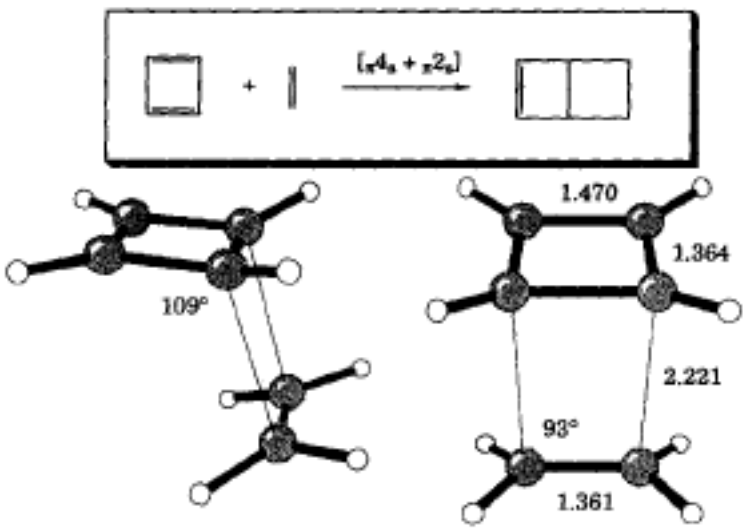

Fig. 46. The RHF/3-21G transition structure of [$_{s}$4$_{s}$ + $_{s}$2$_{s}$] cycloaddition between cyclobutadiene and ethene (Y. Li).

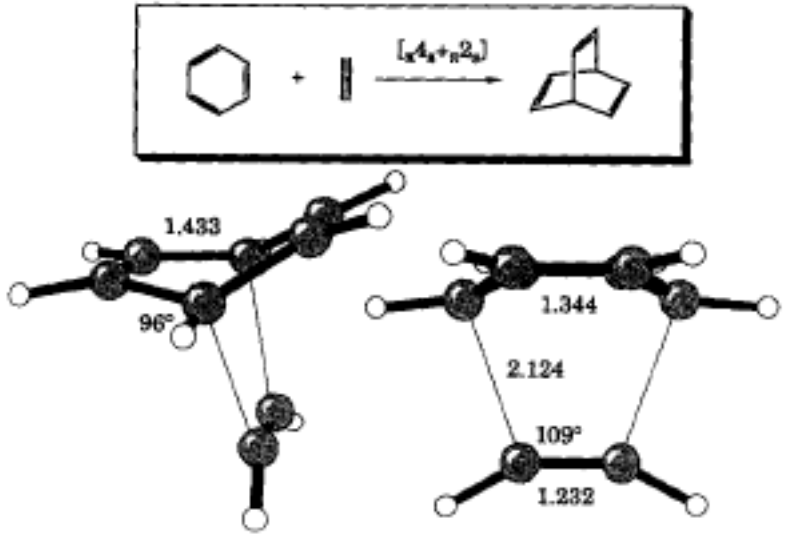

Fig. 48. The RHF/3-21G transition structure of [$_{s}$4$_{s}$ + $_{s}$2$_{s}$] cycloaddition between benzene and acetylene (Y. Li).

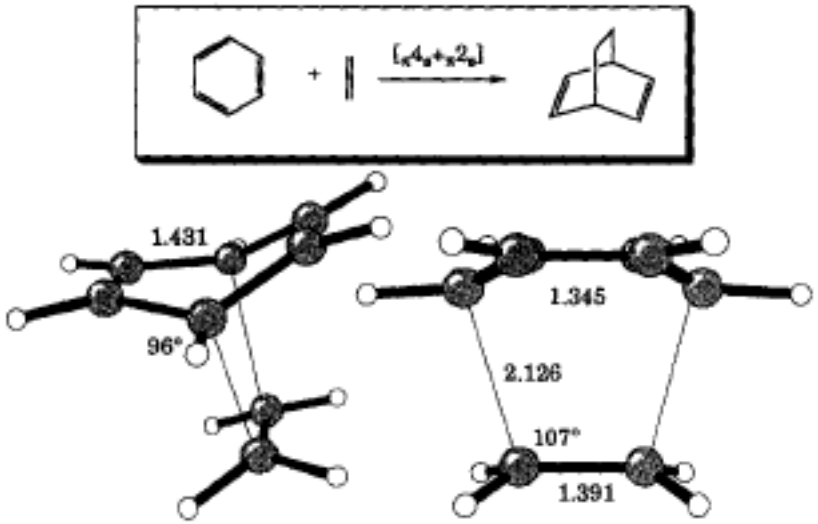

Fig. 47. The RHF/3-21G transition structure of [$_{s}$4$_{s}$ + $_{s}$2$_{s}$] cycloaddition between benzene and ethene (Y. Li).

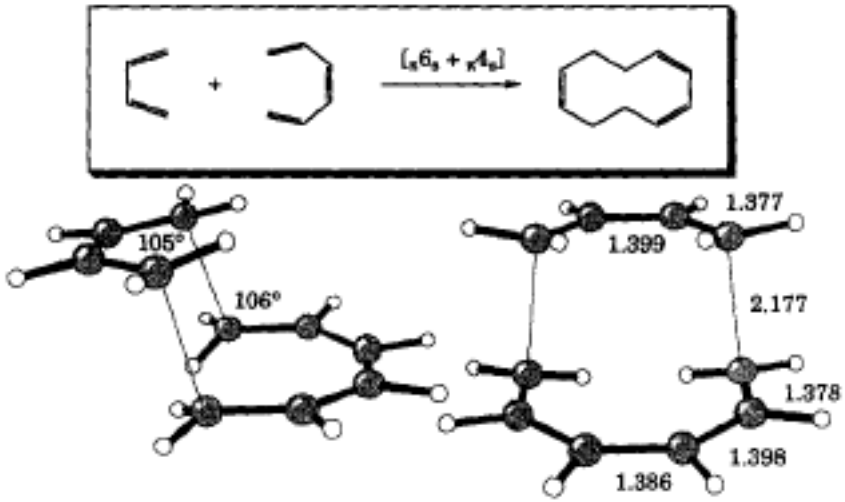

Fig. 49. The RHF/3-21G transition structure of [$_{s}$6$_{s}$ + $_{s}$4$_{s}$] cycloaddition between *cis*-hexatriene and butadiene (Y. Li).

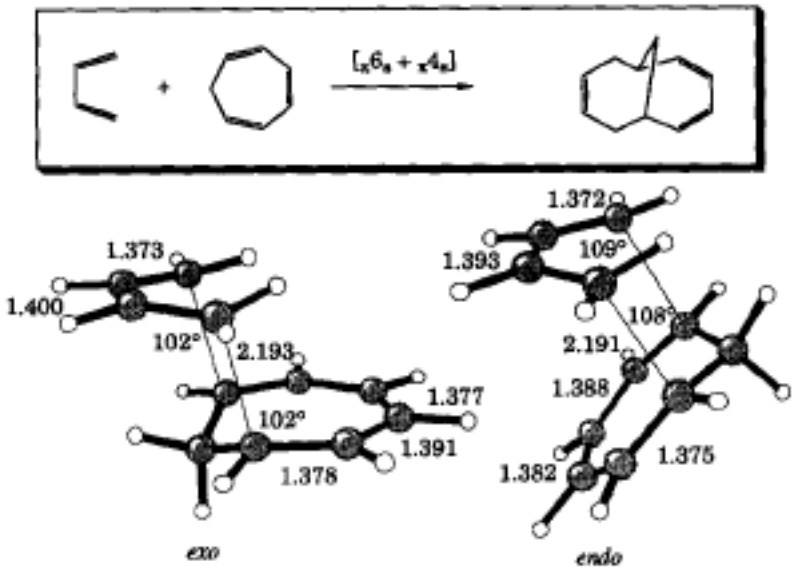

Fig. 50. The RHF/3-21G *exo* and *endo* transition structures of [$_{\pi}6_{s} + {}_{\pi}4_{s}$] cycloaddition between cycloheptatriene and butadiene (Y. Li).

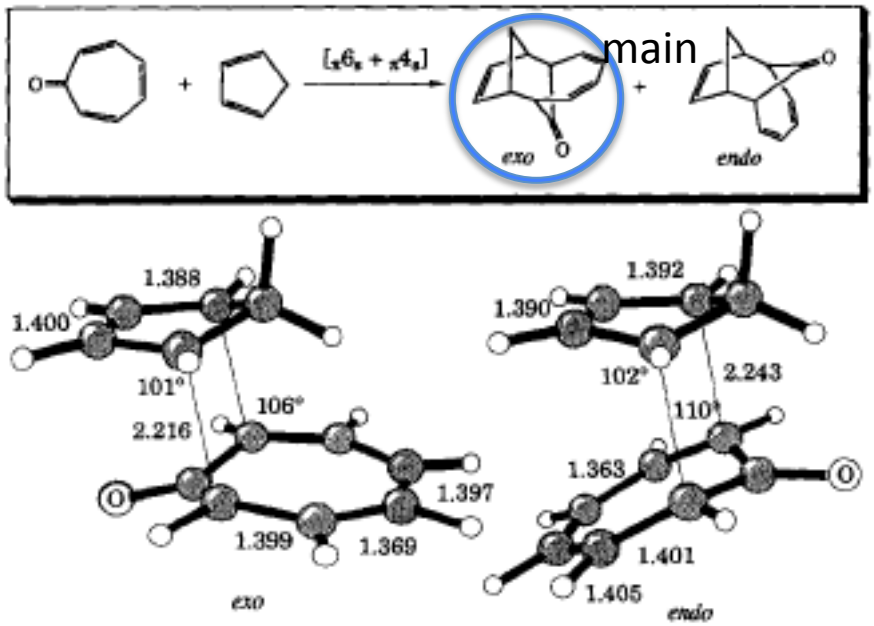

Fig. 51. The RHF/3-21G *exo* and *endo* transition structures of [$_{\pi}6_{s} + {}_{\pi}4_{s}$] cycloaddition between tropone and cyclopentadiene (Y. Li).

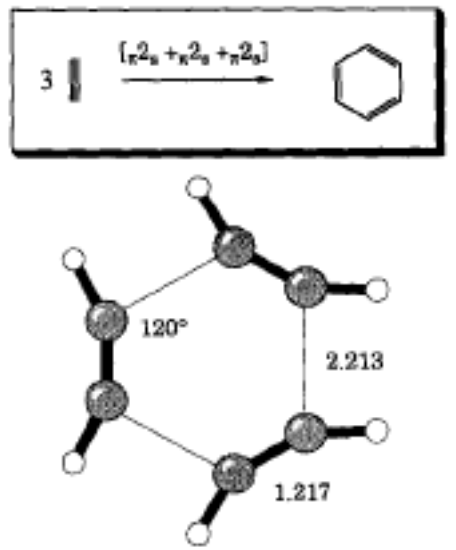

Fig. 52. The RHF/6-31G* transition structure of [$_{\pi}2_{s} + {}_{\pi}2_{s} + {}_{\pi}2_{s}$] cyclotrimerization of acetylene [129b].

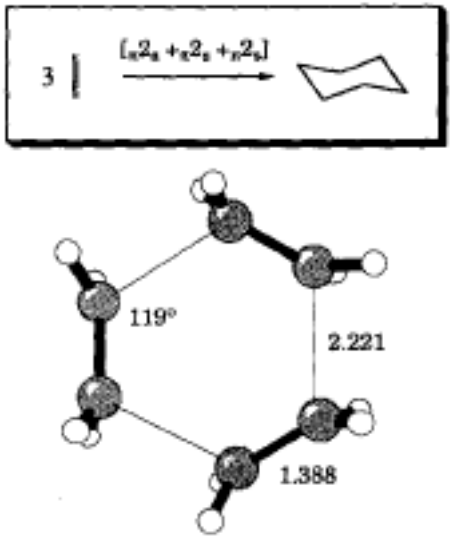

Fig. 53. The MP2/6-31G* transition structure of [$_{\pi}2_{s} + {}_{\pi}2_{s} + {}_{\pi}2_{s}$] cyclotrimerization of ethene (Y. Li).